

Modified Split Hopkinson Pressure Bar adapted to porous and low strength materials testing

Rumen Krastev*, Vasil Kavardzhikov, Tatiana Simeonova
Institute of Mechanics – Bulgarian Academy of Sciences, Sofia, Bulgaria
Email: r_krastev@imbm.bas.bg

Abstract: A modified version of the Split Hopkinson-Kolsky Pressure Bar is described, intended for impact testing of porous metals and other low-strength materials. In it, one bar is made of aluminum alloy and the other bar is a steel tube. Several variants of the mathematical model for working with such devices are described. The stress-strain diagram of the specimen is extracted from the first impact signal. Attention has been paid to the approach to choosing the initial moments from which the calculations must start. Several examples are shown with solid and porous aluminum alloy samples. Despite the lack of high accuracy of the diagram at small stresses, the facility is suitable for quickly obtaining the overall appearance of the diagram after crushing small cylindrical specimens (up to 10 mm in diameter and height) and estimating the stresses at which the material deforms plastically.

Keywords: SPLIT HOPKINSON PRESSURE BAR, DIFFERENT MATERIALS AND CROSS SECTIONS OF INCIDENT AND TRANSMITTED PULSE BARS, POROUS AND LOW-STRENGTH MATERIAL

1. Introduction

The study of the behavior of metal specimens at high deformation rates was started in the second half of the 19th century by John Hopkinson and his son Bertrand Hopkinson, who created the first systems for recording and studying the deformations of specimens under impact loading. The scientific and technological reaches in the middle of the 20th century made possible the systematic and correct measurement and research of the course of the stressed and deformed state of the materials under impact loads. The creator of the system with which these observations and measurements were established is Herbert Kolsky [1]. It was popularized under the name "Hopkinson's Bar" in honor of the initiators of these studies. This system is now known as the "Split Hopkinson-Kolsky Pressure Bar". Kolsky applied it for measurement of the dynamic stress-strain responses of various materials: polymers (polyethylene, polymethylmethacrylate), rubbers (natural and synthetic) and metals (copper, lead).

At the beginning of the new century, advanced technologies for high-speed recording and processing of large data sets were created and became widely available. This stimulated the creation of new modifications of the base system and the expansion of possibilities for dynamic studies of materials under various loading types and speeds [2, 3].

In recent decades, the interest of researchers in the field of materials science has been focused on the development of technologies for creating porous materials. These materials are attractive for engineering practice because they are relatively light (ρ) and have a high ability to deform and absorb kinetic energy upon impact. Hopkinson's bar system is basic for these studies [2, 4, 5, 7]. The main concern in the experiments with this system is to create conditions for obtaining a sufficiently large amplitude of the transmitted pulse when studying such low-strength materials [8, 9].

In the present work, a modification of the Hopkinson bar system is presented, designed for dynamic studies of low-strength materials subjected to impact compression. Results obtained in studying the metrological capacity of this system are reported.

2. Modified Split Hopkinson Pressure Bar adapted to porous and low strength materials testing

Fig. 1 shows one configuration of the Split Hopkinson Pressure Bar, produced by the French company "Thiot Ingenierie".

The bars have a diameter of 20 mm, a length of 2 m each, and are made of Maraging 300 steel. Using strikers up to 800 mm long and impact speeds up to 28 m/s, the equipment is suitable for testing of dense metallic materials with yield strength above 100 MPa. The samples are cylindrical with a diameter and height up to 8 mm.

Interest has been shown in impact testing of porous metallic materials that have a significantly lower yield strength, 10 to 30 MPa. At such stresses, the transmitted deformation pulse is very weak and we doubt the accuracy of the measurement.

Using the experience shared by Chen and other authors [8, 6, 9] we kept the diameter of the cross section and the length of the bars the same as in the system of Fig. 1, but we changed the material from which they are made and for the transmitted pulse "bar" we also use a tube. The new system configuration and additional information about it are presented in Fig. 2. and Table 1.



Fig. 1. A Split Hopkinson Pressure Bar system designed for testing of metals

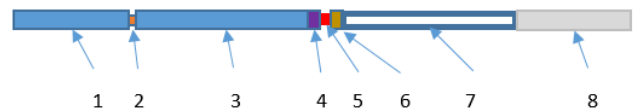


Fig. 2. Scheme of the Split Hopkinson Pressure Bar equipment, modified for testing of low-strength materials

Table 1. Material and dimensions of the elements

Pos.	Designation	Diameter mm	Length mm	Material
1	Striker	18	700	Al D16
2	Shaper	8	1	Washer M4, CuZn
3	Incident bar	20	2000	Al 2024-T3
4	Pad	20	8	Maraging 300
5	Specimen	5 - 10	5 - 10	Porous metal Low strength material
6	Pad	20	8	Maraging 300
7	Transmitted Pulse Tube	$D_o = 20$ $d_i = 12$	1996	St. 45
8	Brake bar	20	1200	Maraging 300

In the middle of round bar 3 and tube 7 there are strain gauges. With the help of high-speed equipment and the mentioned strain gauges, the strain-time diagrams are recorded with a frequency of 1 MHz of the Incident pulse, of the Reflected pulse and of the Transmitted through the specimen pulse. The three log charts are used to calculate the specimen's crush over time.

Such device (with a tube for the transmitted impulse) is suitable for testing of porous materials up to large deformations, as well as for testing dense samples with moderate strength.

To verify this configuration, a comparison was made between diagrams obtained with the original bar configuration

and with the new configuration, on specimens of the same material, Al 2024-T3. A comparison of porous specimens has been made, but their dispersion is quite large, both in static and dynamic tests, and therefore they are not usable as criteria for proving the quality of this equipment.

3. Theory

Theoretical models for Split Pressure Hopkinson Bars made from different materials and with different cross-section are considered below. We use the following indices:

I – refers to the Incident bar or Incident pulse

R – refers to the Reflected pulse recorded by the incident bar sensor

T – refers to Transmitted pulse or the tube, behind the specimen

0 – refers to the initial dimensions of the specimen.

3.1 Simplified model of a typical Hopkinson - Kolsky bar to determine the specimen deformation

In his work Kolsky used the term "pressure", referring to a pulse of compressive stress or tensile stress passing through the bars. Of course, the transfer of this stress pulse is accompanied by a displacement of the bar material, including displacements of the ends of the bars. When strain gauges register a deformation pulse passing under the sensor and we are interested in the displacements of the ends of the bars, then it is more convenient to use formulas relating the recorded deformations to the desired displacements of the ends of the bars. The derivation of the equations for a typical Hopkinson - Kolsky bar (built of cylindrical solid round bars of the same diameter and the same material), which allows calculation of the stress-strain diagrams during crushing of the specimen, can be found in many publications [2], [10], [11].

The engineering stress in the specimen is calculated according to the stress in the transmitted pulse bar, as the force with which the specimen and the tube interact must be equal in magnitude:

$$(1) \quad s(t) = \frac{A_T}{A_0} E_T \varepsilon_T(t)$$

Where t and τ – time, $s(t)$ – calculated engineering stress of the specimen over time, A_T – cross-section of the transmitted pulse bar, E_T – dynamic elastic modulus of the transmitted pulse bar, A_0 – initial cross-section of the specimen, $\varepsilon_T(\tau)$ – dependence of the transmitted deformation pulse on time.

Examining the displacements on both sides of the specimen leads to an equation involving the three recorded dependences of incident, reflected, and transmitted strain pulses over time. Adding the idea of force balance on both sides of the sample (see equation (6)) leads to the so-called simplified equation [2]:

$$(2) \quad e(t) = \frac{-2C_I}{L_0} \int_0^t \varepsilon_R(\tau) d\tau$$

Where $e(t)$ – calculated engineering deformation of the specimen in time, C_I – speed of sound in the incident bar, L_0 – initial height of the specimen, $\varepsilon_R(\tau)$ – dependence of the reflected deformation pulse on time.

3.2 Deformation of the specimen when bars have different cross-sections

Eq. (3) is present in [8] and [6] for the case, when transmitted bar is a tube, and both bars are made of one and the same material.

$$(3) \quad e(t) = \frac{C_I}{L_0} \left(1 - \frac{A_I}{A_T}\right) \int_0^t \varepsilon_I(\tau) d\tau - \frac{C_I}{L_0} \left(1 + \frac{A_I}{A_T}\right) \int_0^t \varepsilon_R(\tau) d\tau$$

Engineering deformation of the specimen is calculated by eq. (3), which takes into account the recorded incident pulse $\varepsilon_I(\tau)$, reflected pulse $\varepsilon_R(\tau)$, cross-section of the incident bar A_I , and the cross-section of the tube for the transmitted pulse, A_T . It is also obtained after "simplification" using a force balance equation (see Eqs. (5), (6)), but considering different cross-

sections of the two bars and the same material (elastic modulus and pulse velocity). This equation is not applicable when the two bars have different material.

3.3 Theoretical model for a SHPB having different bars

The equations for displacements of the contact surfaces of the two bars can be used to obtain the specimen deformation. After considering the displacement velocities of the bar faces on both sides of the specimen, using the typical approach [1], [8], [2], but considering different bars, we arrive to Eqs. (4) and (4a).

$$(4) \quad e(t) = \frac{C_I}{L_0} \int_0^t [\varepsilon_I(\tau) - \varepsilon_R(\tau)] d\tau - \frac{C_T}{L_0} \int_0^t \varepsilon_T(\tau) d\tau$$

$$(4a) \quad e(t) = \frac{C_I}{L_0} \int_0^t [\varepsilon_I(\tau) - \varepsilon_R(\tau) - \frac{C_T}{C_I} \varepsilon_T(\tau)] d\tau$$

Where C_T is the speed of sound in the tube of the passed pulse.

Hereafter we will call equations (4) "primary equations" for calculating the strain of the specimen.

When considering a device with two different bars, having different materials and cross-sections, Eq. (1) still can be used to calculate the stress in the specimen, where A_T is the solid cross-section of the transmitted pulse tube.

3.4 Force balance

Following the sequence in [8], but considering bars of different materials and cross-sections, the condition for force equilibrium on both sides of the specimen can be written as eq. (5):

$$(5) \quad E_I(\varepsilon_I(\tau) + \varepsilon_R(\tau))A_I = E_T \varepsilon_T(\tau) A_T$$

Eq. (6) is obtained when both bars have equal cross-sections and material.

$$(6) \quad \varepsilon_I(\tau) + \varepsilon_R(\tau) = \varepsilon_T(\tau)$$

Pay attention that variable ε_R has a different sign than the other two variables.

Equation (6) is known from Kolsky's article [1, p. 686] and is explained in detail by other authors [2], [10], [11]. Using this equation for bars of the same material and the same cross-section leads to the well-known, simplified Eq. (2).

It is widely assumed that no force equilibrium establishes initially on both sides of the specimen, i.e. equation (6) is not valid and accordingly equation (2) is not accurate for the initial part of the computed diagram.

It is convenient to transform eq. (5) in dimensionless form if we want to check the hypothesis of force equilibrium on both sides of the specimen.

$$(7) \quad B(\cdot) = K_B \frac{\varepsilon_T(\tau)}{\varepsilon_I(\tau) + \varepsilon_R(\tau)}$$

Where

$$(8) \quad K_B = \frac{E_T A_T}{E_I A_I}$$

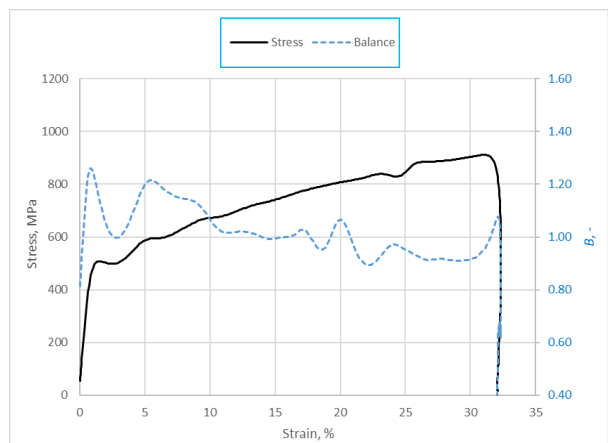


Fig. 3. Engineering diagram and fluctuation of the force balance. Material Al 2024-T3. 5 mm initial diameter and height.

We consider that the value of the variable B (Balance) is close to 1 when force balance is established on both sides of the specimen. In fact, the recorded signals fluctuate and value of the variable B fluctuates around the unit. Fluctuations are notable for dense metallic materials, Fig. 3, and they are very big for porous metallic materials (not shown).

3.5 Equations with two variables

Regardless of the doubts about the validity of the force equilibrium condition at small deformations, it is used to "simplify" the primary equations and this leads to Eq. (2) for identical bars and to Eqs. (4) for bars with different cross-sections. Eq. (9) follows from (7) when we assume a force balance, $B = 1$.

$$(9) \quad \varepsilon_I(\tau) + \varepsilon_R(\tau) = K_B \varepsilon_T(\tau)$$

One of the variables can be eliminated from the system of equations (4) and (9) when we consider a system of different bars. Depending on which variable is eliminated, the following three equations are obtained:

$$(10) \quad e(t) = \frac{C_I}{L_0} \int_0^t \left[\left(1 - \frac{C_T}{C_I K_B}\right) \varepsilon_I(\tau) - \left(1 + \frac{C_T}{C_I K_B}\right) \varepsilon_R(\tau) \right] d\tau$$

$$(11) \quad e(t) = \frac{C_I}{L_0} \int_0^t \left[-2\varepsilon_R(\tau) + \left(K_B - \frac{C_T}{C_I}\right) \varepsilon_T(\tau) \right] d\tau$$

$$(12) \quad e(t) = \frac{C_I}{L_0} \int_0^t \left[2\varepsilon_I(\tau) - \left(K_B + \frac{C_T}{C_I}\right) \varepsilon_T(\tau) \right] d\tau$$

Equations (10), (11) and (12) will be referred to as *two-variable equations* for calculating the strain history. Calculations with them give similar, but different results, because of the different interferences in the signals and the presence of energy losses in the reflected signal.

Using the two-variable equations will give a different deformation than the one calculated by Eq. (4), because they include the idea of force balance at any time.

3.6 Two-variable equations for a classical device

When we consider a classical SHPB, having two bars from the same material and equal diameter, equations (10) – (12) are simplified. It is visible that equations (10) and (11) simplify to eq. (2), but eq. (12) simplifies to eq. (13).

$$(13) \quad e(t) = \frac{2C_I}{L_0} \int_0^t [\varepsilon_I(\tau) - \varepsilon_T(\tau)] d\tau$$

3.7 Selection of the beginning when reading the deformation signals

Experience shows that regardless of the eq. we use: (2), (4), (10) - (13), the resulting *stress-strain* diagram of the specimen is, as a whole, not significantly affected by the points we have chosen to start the calculations.

However, the initial section of the resulting diagram (when deformation and stress are small) strongly depends on the initial moments in the time, which are chosen for the beginning of the calculations (the moments when $\tau = 0$). If we wish the beginning of the diagram to be as reliable as possible, then we must have a well-motivated approach for choosing these moments.

The analysis of data from our device shows that the time from the beginning of $\varepsilon_I(\tau)$ to the beginning of $\varepsilon_R(\tau)$ is not a constant. This time varies from 381 μs to 389 μs with the average being 386 μs . The time from the beginning of $\varepsilon_R(\tau)$ to the beginning of $\varepsilon_T(\tau)$ varies from 2 μs to 15 μs and the average is 8.9 μs . We think that these different time delays are due to different materials, different specimen heights, different quality of the faces of the specimens, and also – different clearances between elements of the system: *Incident_bar-pad-specimen-pad-transmitted_pulse_tube*. These time delays cannot be described theoretically. They could be measured experimentally when we have some well-motivated method for reliable identification of their beginning.

Various approaches have been thought and tried for scientifically based selection of the starting points from which to start the counting of dependencies $\varepsilon_I(\tau)$, $\varepsilon_R(\tau)$ and $\varepsilon_T(\tau)$.

- The simplest approach is to start calculations when the chart begins to deviate from its zero value. This approach can lead to errors due to too early start of counting for the incident pulse, as well as the risk of miscounting the beginning of the reflected pulse due to bars and signal fluctuations.
- A better approach is to choose limits such as 50 $\mu\text{m/m}$ for $|\varepsilon_I|$; 40 $\mu\text{m/m}$ for $|\varepsilon_R|$ and 10 $\mu\text{m/m}$ for $|\varepsilon_T|$, after the passage of which to start counting the dependencies. This approach is better, but the best thresholds depend on the type of material.
- Thresholds, for example, 10% of the highest (absolute) value of the corresponding deformation can be used as a criterion when $\tau = 0$.

Stepping on our experience we accept the last approach for optimal, i.e. to calculate engineering stress and engineering strain histories we start the calculations from the first points near the thresholds 10% $\varepsilon_I(\tau)_{max}$, 10% $\varepsilon_{-R}(\tau)_{max}$ and 10% $\varepsilon_T(\tau)_{flow}$, Fig. 4. Here $\varepsilon_T(\tau)_{flow}$ is a point in the diagram, after which intensive plastic flow is visible.

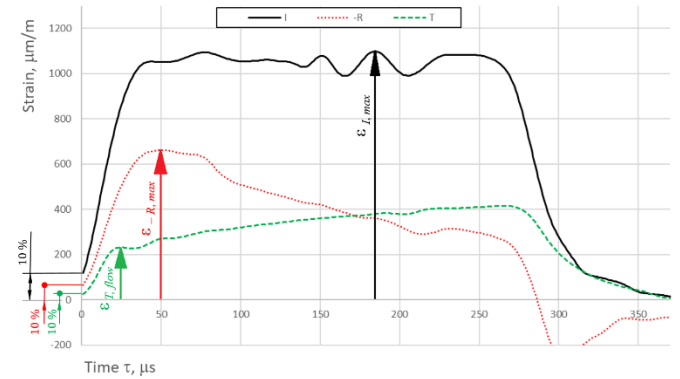


Fig. 4. Selection of the moments for the start of the calculations, using the 10% approach.

4. Experimental part

4.1 Experimental plan

The report shows a comparison of experimental impact test results of identical Al 2024 T3 specimens tested with the original bar configuration, Table 2, and tested with the new configuration of the facility, Tables 1 and 3.

4.2 Equipment

Table 2. Original SHPB configuration

Property	Value	Unit
Material	Maraging 300	
Diameter	19.94	mm
Length (incident bar, transmitted pulse bar)	2000	mm
Elastic modulus	180.6	GPa
Speed of sound C_I , C_T	4730	m/s

Table 3. Modified SHPB configuration

Property	Value	Unit
Incident bar		
Elastic modulus, E_I	78.2	GPa
Speed of sound, C_I	5220	m/s
Transmitted pulse tube		
Elastic modulus, E_T	209	GPa
Speed of sound, C_T	5155	m/s
Balance constant K_B		
	1.7422	-

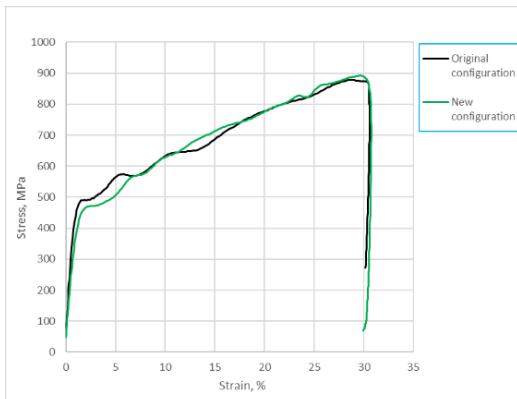


Fig. 5. Comparison the average diagrams of equal specimens (Al 2024-T3, $d_o=8$ mm, $h_o=8$ mm), obtained using the original and the new configuration

Recorded signals were exported as text files and were processed in Excel. Deformation was calculated according to Eq. (12) unless otherwise stated in the description.

Strain signals obtained from the original equipment are filtered in Excel using the *moving-average* method, with period $k = 11$, (averaging of five values from each side). Strain signals obtained from the modified equipment are filtered by the recording device, using an integrated low pass filter *Bessel 6th order*, 40 kHz.

4.3 Experimental results

See Figs. 5 and 6.

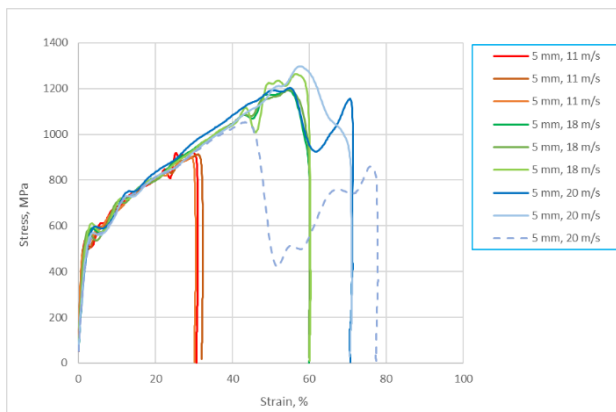


Fig. 6. Engineering diagrams obtained for material Al 2024-T3, 5 mm initial diameter and height, tested with different impact velocities on the new SHPB

5. Discussion

We have a Split Hopkinson Pressure Bar designed for high-speed impact testing.

In order to test weak materials, the available equipment was modified as the incident bar was made of solid Al 2024-T3, and a St. 45 tube was used to measure the transmitted pulse. A mathematical model necessary for the correct interpretation of the signals in this configuration (solid incident bar and transmitted pulse tube of different materials) was developed.

The engineering stress is calculated by the typical formula, eq. (1), having in mind that cross area and elastic modulus are related to the transmitted pulse tube.

We also consider the idea of force balance on both sides of the specimen, thinking for an arbitrary SHPB device, see Eqs. (7), (8) and Fig. 3. This idea in combination with the classical eq. for the engineering deformation (eq. (4)), leads to a set of three two-variable equations, (10) – (12). Our experience shows that reflected pulse has unwanted fluctuations and usually it is a little smaller than theoretically expected due to loss of energy. That is why we prefer to use eq. (12) for calculation of the engineering strain. This equation simplifies to eq. (13) when we consider a classical SHPB (equal materials and cross-section of the both bars).

The practice shows that diagrams have lower dispersion when we start the calculations after reaching a relatively stable compression condition over the specimen. At this time we assume

that the mentioned condition represents well mathematically with three thresholds: $10\% \varepsilon_I(\tau)_{max}$, $10\% \varepsilon_{-R}(\tau)_{max}$ and $10\% \varepsilon_T(\tau)_{flow}$, Fig. 4. Here $\varepsilon_T(\tau)_{flow}$ is a point in the diagram, after which intensive plastic flow is visible. In this way, the time τ has to be counted from a point (in the table data) that is close to or after these thresholds.

Tests were made on identical specimens with the original device and with the modified device. The data are shown and compared in Fig. 5. It can be seen that the mean diagrams obtained for the two configurations of the Hopkinson bar coincide, although they were calculated by different formulas (Eq. (1) and Eq. (13) for the experiments performed with the original configuration; Eq. (1) and Eq. (12) with the coefficients from Table 3, for the experiments made with the new configuration). This proves that the methodology used is correct and the new bar configuration can be relied upon using the described methodology for calculating the charts.

It can be seen in Fig. 6 that diagrams of the specimens are quite close up to 45% strain and engineering stress up to 1000 MPa. All three specimens that were impacted at 20 m/s fractured (a sharp change in the diagram is seen) with the engineering stress at fracture ranging from 1100 to 1300 MPa.

6. Conclusions

1. Equations (10), (11), (12) are derived for obtaining the specimen deformation, tested on arbitrary configurations of Hopkinson bars (made of different materials and with different cross-sections).

2. We consider that Eq. (12) is preferable to use because it does not contain the reflected deformation pulse $\varepsilon_R(\tau)$, which contains rather large fluctuations and has energy loss in its creation.

3. Experimental data show that moments to start calculations (when $\tau = 0$) influence the beginning of the obtained diagrams. This issue was considered in section 3.7. Additional analyses may be performed, but our experience so far led to the “10% approach” explained in Fig. 4 and the surrounding text.

4. The modified Hopkinson bar can be used with the methodology developed for testing dense materials (recommended diameter and height of 5 mm) and for testing porous materials (diameter and height up to 10 mm).

7. Funding

This work is supported by the European Regional Development Fund within the OP Science and Education for Smart Growth 2014–2020, Project CoE “National Center of Mechatronics and Clean Technologies”, BG05M2OP001-1.001-0008.

This research was funded by the Bulgarian National Science Fund, Project **KII-06-H57/20** “Fabrication of new type of self-lubricating antifriction metal matrix composite materials with improved mechanical and tribological properties”.

8. References

1. **Kolsky H.** An Investigation of the Mechanical Properties of Materials at very High Rates of Loading. Proc. Phys. Soc. Lond. B 62 (1949) 676–700
2. **Chen Weinong, Bo Song.** Split Hopkinson (Kolsky) Bar. Design testing and applications. Springer (2011) pp. 3-27
3. **Gilat Amos, Jeremy D. Seidt.** Compression, Tension and Shear Testing of Fibrous Composite with the Split Hopkinson Bar Technique, EPJ Web of Conferences 183, 02006 (2018)
4. **Kim Selim, Dong Geun Kim, Minu Kim, et al.** Analyses of impact energy-absorbing performance of open- and closed-cell Al foams using modified split Hopkinson pressure bar, Journal of Alloys and Compounds 965 (2023) 171349, pp. 2-12
5. **Jing, Lin, Xingya Su, F. Yang, et al.** Compr. strain rate dependence and constitutive modeling of closed-cell aluminum foams with various relative densities, J. Mater. Sci. 53 (2018) 14739-14757

6. **Raj. R. Edwin, Venkitanarayanan Parameswaran, B.S.S. Daniel.** Comparison of quasi-static and dynamic compression behavior of closed-cell aluminum foam. *Materials Science and Engineering A* 526 (2009) 11–15
7. **Xie, Beixin, Liqun Tang, Yiping Liu, Zhenyu Jiang and Zejia Liu,** Numerical Analysis on Usability of SHPB to Characterize Dynamic Stress–Strain Relation of Metal Foam, *International Journal of Applied Mechanics*, Vol. 9, No. 5 (2017) 1750075
8. **Chen W., B. Zhang, MJ Forrestal.** A Split Hopkinson Bar Technique for Low-impedance Materials, *Experimental Mechanics*, Vol. 39, No 2, June 1999 (81-85).
9. **Chen, Longyang, Hui Guo, Weiguo Guo et al.** Research on Several Problems in the Characterization of Lightweight Cellular Materials by Low-Impedance Hopkinson Pressure Bar, *Journal of Testing and Evaluation*, Vol. 48 No. 6 (2020)
10. **Lindholm, U.S.** Some experiments with the Split Hopkinson Pressure Bar. *J. Mech. Phys. Solids*, 1964, Vol. 12, pp. 317-335. Pergamon Press Ltd. Printed in Great Britain
11. **Ramesh, Kalias T.** Chapter 33 - High Rates and Impact Experiments - in: *Springer Handbook of Experimental Solid Mechanics*. Springer, Berlin, Germany, (2008); pp. 929-959.